

Solving Path Following Problem for Car-Like Robot in the Presence of Sliding Effect via LMI Formulation

Masoud Emam, Ahmad Fakharian *

Faculty of Electrical, Biomedical, and Mechatronics Engineering, Qazvin Branch, Islamic Azad University, Qazvin, Iran

Received 6 March 2017; revised 31 August 2017; accepted 19 September 2017; available online 16 October 2017

Abstract

One of the main problems of car-like robot is robust path following in the presence of sliding effect. To tackle this problem, a robust mix H_2/H_∞ static state feedback control method is selected. This method is the well-known linear robust controller which is robust against external disturbance as well as model uncertainty. In this paper, the path following problem is formulated as linear matrix inequality for the kinematic model of car-like robot, which includes sliding effect. The robustness and path following performance of the proposed controller are investigated based on the comparison of suggested controller with an optimal proportional integral controller. The simulation results, which have been performed by MATLAB Simulink, shows the presented controller is able to follow various paths including simple, linear and more complex function path like square, and sine function path even in the presence of sliding effect. In addition, the robustness and correctness of closed-loop system in the simulations are demonstrated based on the nonlinear analysis of equilibrium point.

Keywords: Car-Like Robot, Path Following Problem, Linear Matrix Inequalities (LMI), Mix H_2/H_∞ Controller.

1. Introduction

Although trajectory tracking is the well-known method to design navigation system for autonomous mobile robots, path following is an alternative approach to design it with some advantages in comparison with trajectory tracking. For instance, turning back is the phenomenon of trajectory tracking that could be eradicate by using path following. Since in trajectory tracking desired robot route is defined as a time function and in each moment only one point's characteristics of route is sent to navigation system as the target point, if the robot is initiated on the middle of desired route it will turn back to go to the start point of desired route; this phenomenon is called turning back. On the other hand, in path following, desired route is defined as a Path, which

is time independent function. Thus, path is sent to navigation system completely, rendered by this system to find closest point, after that robot tends to nearest point of the path, and eventually follows the path after reaching it. As a result, turning back is impossible. It is worth noting that, presented process of path following is the most common approach to solve path following problem, which is also used in this article, called 'virtual target tracking'. Although this approach is not the only technique to solve path following problem, other approaches result the same advantage as well.

Over the recent years, plenty of research have been done in the field of path following problem for navigation of autonomous robots or vehicles and researchers have

* Corresponding author. Email: ahmad.fakharian@qiau.ac.ir

designed various controllers from linear and nonlinear classic controllers to intelligent and fuzzy controllers. Feedback linearization is one of the most common nonlinear controller design method that is used in [1]. In this research, a car-like robot parallel parking is defined as path following problem and it is solved by feedback linearization and Sliding Mode Control (SMC) method. Note that in [1], sliding effect is not taken into the account. Moreover, a modification of feedback linearization which is called transverse feedback linearization is used in [2] and [3] to navigate a car-like robot in non-sliding environment. It is important to note that, since under real circumstances existence of sliding effect is inevitable, the controllers that are presented in [1-3] are not able to implement. Another nonlinear method is used in [4], is adaptive backstepping. Although in [4] side-slip friction is taken into account, due to utilizing dynamic model of car-like robot and nonlinear controller design method, designing procedure as well as resulting controller are more complex than the suggestion of this paper.

Intelligent methods are used in some researchs. In [5], the authors presented fuzzy PID controller to solve the path following problem for a car-like robot. In addition, a novel method is used in [6]. In [6], amount of sliding effect is estimated by an intelligent system which analyzes vision system images to do this estimation. It is worth noting that, not only is path following used to design navigation system for the car-like robot, but it is also applied to other robots and vehicle like: quadrotor [7] and marine vehicles [8].

Robust path following control of car-like robot is one of the most common technique to design these controllers due to the presence of sliding effect. In sliding situation, if the robot is not controlled by a robust controller, which has robustness to sliding effect, it will follow the path with high position error. Numerous articles have been published in the field of robust path following of car/car-like robot which are investigated in the following. In [9] and [10], robust H_∞ controller is designed by Linear Matrix Inequality (LMI) approach. This controller has been chosen to benefit robustness against model uncertainty as well as external disturbance. Note that, in this article dynamic model of car vehicle has been used as the system model and simulations have been done by CarSim-Simulator. Since using dynamic model to take sliding effect into the account causes some complexity and nonlinearity, in this kind of article, which uses dynamic model, steering angle variation is considered

just around zero to linearize and deal with this complexity. So, in this article we chose kinematic model of car like robot to avoid of this assumption which is not accurate enough.

In [11], robust L_∞ controller is designed for kinematic model of car-like robot and authors of [11] have proven that this controller could navigate car-like robot even in the presence of sliding effect. Furthermore, they used LMI to solve their control problem. This paper is one of the best research in the field of car-like robot path following because the authors removed all the shortages that are mentioned before about [1-4] and [9, 10]. It is worth noting that, all of these advantages including designing simple robust controller, utilizing kinematic model of car-like robot which includes sliding effect, and defining the path following problem as LMI formulation are in the same with advantages that we attained in this paper. But, since we designed a mix robust controller, more advantages are achievable such as low energy control signal, and robustness against both low and high frequency change in amount of sliding effect angle.

In this paper, we design a robust H_2/H_∞ static state feedback controller to solve car-like robot path following problem by LMI approach. Mix H_2/H_∞ controller is benefited from advantages of both H_∞ and H_2 controllers, since this mixed controller is designed by taking constraints of both controllers into the account simultaneously. H_∞ controller is a well-known robust controller with robustness against low frequency disturbances including: model uncertainty and external disturbances, but usually the control effort of this controller is high and in a few cases because of control effort this controller is not implementable. On the other hand, H_2 controller is another common robust controller with robustness against high frequency disturbances such as measurement noise. By utilizing this controller it is possible to decrease energy of some internal signal of controlled system such as control signal, because H_2 controller limits H_2 -Norm (H_2 -Norm of a system represents the energy) of a sub-system of controlled system. Therefore, as the main contribution of this paper, this control method is selected to achieve the robustness against both low frequency and high frequency disturbance as well as low energy control signal which results a robust controller to navigate a car-like robot in the presence of sliding effect and implementable controller because of low energy control signal. In addition, an optimal Multi-Input Single-Output (MISO) Proportional-Integral (PI) controller is designed utilizing Genetic Algorithm (GA), which is a well-known

control method, to compare with the suggestion of this paper and to prove the accurate response of suggested controller.

The remaining parts of this article is classified as following. First, mathematical modelling of car-like robot kinematic and path following problem will be presented in Section II. Then in Section III, robust static state feedback mix H_2/H_∞ controller as well as MISO PI controller will be developed. Next, simulation results will be exhibited in Section IV. Finally, Section V is devoted to conclusion.

2. System Modelling And Problem Statement

2.1. Kinematic Model of Car-Like Robot

In this article, a well-known car-like robot is considered with rear driving wheels and front steering which is shown in Figure 1. Kinematic model of this robot usually is presented by bicycle model (1) [11].

$$\begin{cases} \dot{x} = v \cos \theta \\ \dot{y} = v \sin \theta \\ \dot{\theta} = v \frac{\tan \phi}{L} \\ \dot{\phi} = \omega \end{cases} \quad (1)$$

Where x and y represent the position of center of rear axis, θ is robot heading angle, ϕ is steering angle, L is distance between front and rear axis, and ω , v are steering angular velocity and robot longitudinal velocity.

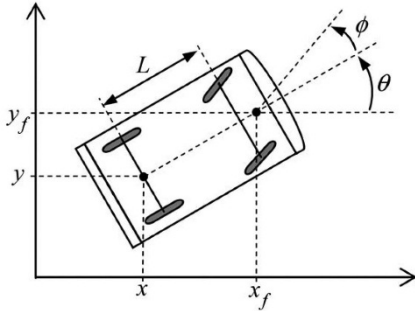


Fig. 1. Car-like robot schematic [11]

It is worth noting that, maximum curvature (κ_{max}) of the desire path is limited due to physical limitation of car-like robot. This limitation is depends on L and maximum possible steering angle (ϕ_{max}) and could be calculated by (2).

$$\kappa_{max} = \frac{\tan \phi_{max}}{L} \quad (2)$$

Since the target of this article is to design a robust controller for car-like robot in the presence of sliding effect, kinematic model of the robot in this circumstance is presented as (3) [11].

$$\begin{cases} \dot{x} = v(\cos \psi_h - \tan \alpha_1 \sin \psi_h) \\ \dot{y} = v(\sin \psi_h + \tan \alpha_1 \cos \psi_h) \\ \dot{\psi}_h = v \left(\frac{\tan(\phi - \alpha_2) - \tan \alpha_1}{L} \right) \\ \dot{\phi} = \omega \end{cases} \quad (3)$$

Note that in previous equations, α_1 and α_2 are sliding angle of rear and front axis respectively (for more details please refer to [11] and [12]).

2.2. Path Following Model

Path following dynamic model of car-like robot consists of two states including e and ψ which are lateral distance between robot center of gravity and closest point of path (T) and angular deviation between robot heading (θ) angle and desire angle of path (ψ_d) at the point T , respectively. This dynamic model is defined as (4) [13].

$$\begin{cases} \dot{e} = v_x \sin \psi + v_y \cos \psi \\ \dot{\psi} = r - \rho(\sigma)v_x \end{cases} \quad (4)$$

Where, v_x and v_y are robot longitudinal and lateral velocity, r is robot yaw rate, and $\rho(\sigma)$ is curvature of desire path at the point T . Note that, robot yaw rate is defined as $r = \dot{\theta}$, angular error is $\psi = \psi_h - \psi_d$, and $\psi_h = \theta$.

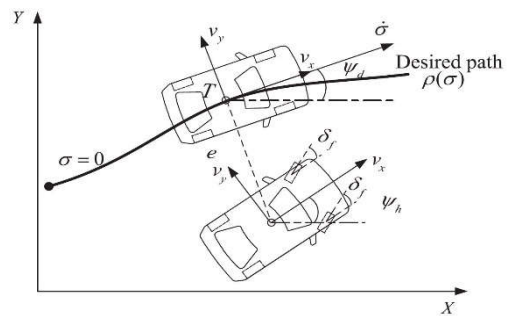


Fig. 2. Path following schematic [13]

In addition, lateral velocity of car-like robot with respect to sliding angle of wheels is defined as (5).

$$v_y = v_x \tan \alpha_1 \quad (5)$$

Eventually, path following model is completed by combining (3), (4), and (5) as following.

$$\begin{cases} \dot{e} = v_x \sin \psi + v_x \tan \alpha_1 \cos \psi \\ \dot{\psi} = v_x \frac{\tan(\varphi - \alpha_2) - \tan \alpha_1}{L} - \rho_{(\sigma)} v_x \end{cases} \quad (6)$$

2.3. Problem Statement

Path following problem for a car-like robot, which is formulated as (6), could be solved by using a controller that asymptotically stabilizes the states of path following model ($[e\psi]$). Since the states of this model are path following errors, asymptotical stabilization of path following model will lead to asymptotic tendency of the robot to desired path.

However, due to the presence of sliding effect, it is possible that non-robust controllers lead to instability, oscillation, and/or steady state error. Therefore, in this article to deal with this difficulty H_2/H_∞ controller, which is a robust controller, is designed.

3. Controller Design

As it mentioned before, in this paper a robust controller is designed to solve path following problem for a car-like robot. We used the static sate mix H_2/H_∞ feedback controller in our design, which is a well-known robust controller with robustness to model uncertainty, external disturbance, and measurement noise. Moreover, this controller is designed by LMI toolbox in MATLAB software. In addition, an optimal MISO PI controller is designed to be compared with mixed H_2/H_∞ controller. These two controllers designing procedures will be presented in detail.

Path following model (6) is considered as the system to design the controller. In detail, this system is governed by steering angle (θ) and robot longitudinal velocity (v_x), $[e\psi]$ is also considered as output signal. In addition, $\rho_{(\sigma)}$, α_1 , and α_2 are unknown parameter. It is worth noting that, curvature $\rho_{(\sigma)}$ is a positive index and has an upper limit based on physical limitation of robot, and $-\pi/2 < \alpha_i < \pi/2$. Thus, if these three unknown parameters are considered as external disturbance owing to using H_∞ controller (as a component of mix H_2/H_∞), since these disturbances are bounded, system is stable even in the presence of this disturbance based on *Small Signal Theorem*.

3.1. Mix H_2/H_∞ Controller (Theories)

In this section fundamental theorem of H_2 and H_∞ static sate feedback controller design based on LMI approach as well as method of mixing these two controllers are presented.

Consider following linear state space representation which is the standard form of system in LMI approach.

$$\begin{cases} \dot{X} = AX + B_1W + B_2U \\ Z_\infty = C_1X + D_{11}W + D_{12}U \\ Z_2 = C_2X + D_{22}U \end{cases} \quad (7)$$

Where, A, B_i, C_j , and D_{ji} are system matrixes, X, U , and W are state vector, system inputs vector, and disturbances vector, respectively. In addition, Z_∞ and Z_2 are performance outputs which are used to define control objectives in H_∞ and H_2 controllers.

Eventually, closed-loop system is calculated as (8) by defining control signal as $U = KX$. Note that, K is a time invariant numerical matrix with appropriate size.

$$\begin{cases} \dot{X} = (A + B_2K)X + B_1W \\ Z_\infty = (C_1 + D_{12}K)X + D_{11}W \\ Z_2 = (C_2 + D_{22}K)X \end{cases} \quad (8)$$

Theorem 1. *H_∞ Controller design.* System (8) is asymptotically stable and infinity norm of the transfer function T , from W to Z_∞ , is less than positive real value γ ($\|T_{W \rightarrow Z_\infty}\|_\infty < \gamma$), if and only if matrix inequality (9) is feasible.

$$\begin{cases} \left(\begin{array}{ccc} (A + B_2K)P_{cl} + P_{cl}(A + B_2K)^T & B_1 & P_{cl}(C_1 + D_{12}K)^T \\ B_1^T & -I & D_{11}^T \\ (C_1 + D_{12}K)P_{cl} & D_{11} & -\gamma^2 I \end{array} \right) < 0 \\ P_{cl} = P_{cl}^T > 0 \end{cases} \quad (9)$$

Theorem 2. *H_2 Controller design.* System (8) is asymptotically stable and second power of 2-norm of the transfer function T , from W to Z_2 , is less than positive real value ν ($\|T_{W \rightarrow Z_2}\|_2^2 < \nu^2$), if and only if matrix inequality (10) is feasible.

$$\begin{cases} \begin{pmatrix} (A + B_2K)P_{cl} + P_{cl}(A + B_2K)^T & B_1 \\ B_1^T & -I \end{pmatrix} < 0 \\ \begin{pmatrix} Q & (C_2 + D_{22}K)P_{cl} \\ P_{cl}(C_2 + D_{22}K)^T & P_{cl} \end{pmatrix} > 0 \\ \text{Trace}(Q) < v^2 \\ P_{cl} = P_{cl}^T > 0 \end{cases} \quad (10)$$

Theorem 3. *Mixed H_2/H_∞ controller design.* System (8) is asymptotically stable, $\|T_{w \rightarrow z_\infty}\|_\infty < \gamma$, and $\|T_{w \rightarrow z_\infty}\|_2^2 < v^2$; if and only if matrix inequalities (11) is feasible.

$$\begin{cases} \begin{pmatrix} Q & (C_2 + D_{22}K)P_{cl} \\ P_{cl}(C_2 + D_{22}K)^T & P_{cl} \end{pmatrix} > 0 \\ \text{Trace}(Q) < v^2 \\ \begin{pmatrix} (A + B_2K)P_{cl} + P_{cl}(A + B_2K)^T & B_1 & P_{cl}(C_1 + D_{12}K)^T \\ B_1^T & -I & D_{11}^T \\ (C_1 + D_{12}K)P_{cl} & D_{11} & -\gamma^2 I \end{pmatrix} < 0 \\ P_{cl} = P_{cl}^T > 0 \end{cases} \quad (11)$$

For more details and proof of the **Theorem 1**, **Theorem 2**, and **Theorem 3** please refer to [14].

3.2. System linearization

According to previous section, to design mix H_2/H_∞ controller system model must be represented in the form of (7). Since this form is linear, path following model (6) must linearize in first step, and then is reorganized to fit to standard form (7).

Linear representation of path following model is calculated by Jacobian method around the equilibrium point of system $[e_{eq} \ \psi_{eq}] = [0 \ 0]$ is (12).

$$\begin{cases} \dot{e} = v_x \psi + v_x \alpha_1 \\ \dot{\psi} = \frac{v_x}{L} \varphi + \frac{v_x}{L} (\alpha_2 - \alpha_1) - \rho(\sigma) v_x \end{cases} \quad (12)$$

Finally, by defining states vector as $X = [e \ \psi]^T$, the system input as $U = \varphi$, external disturbance vector as $W = [\alpha_1 \ \alpha_2 \ \rho(\sigma)]^T$, performance outputs as $Z_\infty = X$, and $Z_2 = [X \ U]^T$ system will be represented in form of (7). For more details and mathematical calculation of finding the equilibrium point and system linearization, readers are referred to **Appendix A**.

It is worth noting that, cause of defining performance outputs in this way is the fact that consideration of states in both performance outputs benefits robustness to high and low frequency external disturbances. Since frequency of external disturbance in this system is unknown and degree of sliding effect could vary slightly or rapidly, robustness to

both kind of disturbance is required. Furthermore, including input signal in Z_2 causes a decrease in energy of control signal (control effort) and prevents sudden changes in control signal, which is usually simultaneous with high amplitude external disturbance or large initial conditions.

3.3. Mix H_2/H_∞ controller for path following of car-like robot

In this article, mix H_2/H_∞ controller is in the form of

$$\left\{ \begin{array}{l} \text{Minimize } \alpha \|T_{w \rightarrow z_\infty}\|_\infty^2 + \beta \|T_{w \rightarrow z_2}\|_2^2 \\ \text{S. t. } \end{array} \right. \quad (9) \quad (13)$$

Where $\alpha = 10$ and $\beta = 1$. In addition, this problem is solved by “*LMI Control Toolbox*”[15] in MATLAB software.

Table. 1. Car-Like Robot Parameters

Parameter name	Parameter value
L	0.2 m
V_x	1 m/s

Note that, in this article longitudinal velocity v_x is constant, like numerous articles in this field such as [11, 13]. This consideration is in order to assuming there exists a low level controller to manipulate the robot dynamics and to keep this velocity constant [16].

The result of static state Mix H_2/H_∞ feedback controller problem (13) calculated by LMI Toolbox for the system (12) with parameters from Table 2 is presented as following.

$$K = (-2.7381 \quad -2.0772)$$

Moreover, H_∞ performance of closed-loop system with this controller is 1.1 and H_2 performance of closed-loop system is 4.07.

3.4. Optimal PI Controller Design

Although PI controller is one of the most common controller in robotic application, there are limited number of research that utilized PI controller for path following of car-like robot. For instance in [5], a fuzzy Proportional-Integral-Derivative (PID) controller is utilized to design path following controller for a car-like robot, but sliding effect does not take into the account and the feedback from car-like robot is position error, only. So, this PID controller is Single-Input Single-Output (SISO) controller. However, in this

paper a MISO PI controller is presented which is optimized by GA.

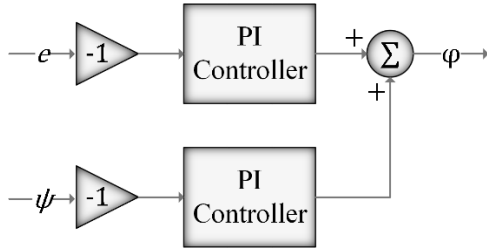


Fig. 3. MISO PI controller structure

The proposed MISO PI controller of this paper consists of two normal PI in parallel structure as it shown in 0. Furthermore, complete equation of MISO PI controller could be defined as (14).

$$\varphi = P_1(-e) + I_1 \int (-e)dt + P_2(-\psi) + I_2 \int (-\psi)dt \quad (14)$$

Note that in (14), P_i and I_i are proportional and integral gains of the i^{th} controller respectively.

Since the quality of PI controller's operation depends on proper choice of controller gains, in this paper, GA is utilized to achieve the best performance of this controller. Moreover, in order to decrease the amount of position error, the cost function that is minimized by GA is defined as (15).

$$J \triangleq \int_0^T e_{(t)} dt \quad (15)$$

To solve GA with cost function (15) MATLAB optimization toolbox has been used with setting parameters that are presented in Table 2 and the optimum resulting controller parameters are presented in Table 3.

Table 2. Setting Parameters of GA

Parameter	Value	
Population	50	
Crossover Operation	none	
Reproduction	Elite count	1
	Crossover fraction	0.8
Mutation Operation	Function	Gusian
	Scale	1
	Shirink	1

Table 3. Optimal Values of Pi Controller Parameters

parameter	value
P_1	1.6390
I_1	0.0230
P_2	39.5204
I_2	11.6124

3.5. Stability Analyze of Closed-Loop System

First and fundamental performance of any closed-loop system undoubtedly is stability. Thus, stability analyze is the first investigation that must be done for controlled car-like robot by the suggested controller of this paper. On the other hand, to proof the success of path following controller in navigation three main ability of controller must be proven. The first requirement is that; the controller must be able to manipulate the robot in a way that robot converges to desired path, if it was not initiated on the path. The second; when the robot reaches to desired path follows it for all the time after reaching. And the third; the robot must never leave desired path after reaching to it. Since the states of system (6) contain position error (distance to desired path), all of the above statements could be translated to stability analyze as **Theorem 4**.

Theorem 4. If closed-loop car-like robot system has a stable equilibrium point X_{eq} which containse = 0, for all initial conditions of this system X_0 that $X_0 \in \mathcal{D}_{X_{eq}}$ ($\mathcal{D}_{X_{eq}}$ is the domain of attraction of X_{eq}) we have:

1. For any initial conditions, robot converges to desired path when the time tends to infinity.
2. After convergence, robot follows desired path.
3. Robot never leaves desired path after reaching it.

Proof: since e is one of the system states and $e = 0$ is stable equilibrium point of the system, according to Lyapunov stability theorem, if $X_0 \in \mathcal{D}_{X_{eq}}$ then e converges to origin when time tends to infinity, after convergence e remains at origin and never leaves there.

In following, it is shown that, the point $[e \ \psi] = [0 \ -\alpha_1]$ is the stable equilibrium point of the closed-loop system of car-like robot to prove the path following ability of the suggested controller based on **Theorem 4**.

By defining $\varphi = k_1 e + k_2 \psi$ the closed-loop system of car-like robot path following (6) is calculated as (16).

$$\begin{cases} \dot{e} = v_x \sin \psi + v_x \tan \alpha_1 \cos \psi \\ \dot{\psi} = v_x \frac{\tan(k_1 e + k_2 \psi - \alpha_2) - \tan \alpha_1}{L} - \rho_{(\sigma)} v_x \end{cases} \quad (16)$$

Now, (16) is linearized system around the point $[e \ \psi] = [0 \ -\alpha_1]$.

$$J = \begin{bmatrix} \partial \dot{e} / \partial e & \partial \dot{e} / \partial \psi \\ \partial \dot{\psi} / \partial e & \partial \dot{\psi} / \partial \psi \end{bmatrix} = \begin{bmatrix} 0 & J_1 \\ J_2 & J_3 \end{bmatrix}$$

Where,

$$J_1 = v_x \cos(\alpha_1) + v_x \tan(\alpha_1) \sin(\alpha_1)$$

$$J_2 = \frac{v_x k_1}{L} (\tan^2(-k_2 \alpha_1 - \alpha_2) + 1)$$

$$J_3 = \frac{v_x k_2}{L} (\tan^2(-k_2 \alpha_1 - \alpha_2) + 1)$$

According to physical limitation of car-like robot and results of controller designing procedure we have: $v_x = 1$, $L = 0.2$, $-\pi/2 < \alpha_i < \pi/2$, $k_1 = -2.7381$, and $k_2 = -2.0772$.

Therefore, it is easily calculated that for any α_i , J is Hurwitz and the point $[e \ \psi] = [0 \ -\alpha_1]$ is the stable equilibrium point of the closed-loop system of car-like robot. To prove this claim, real component of the two Eigen values of the matrix J are plotted in 0 and 0 in terms of different values of α_1 and α_2 . As shown in these figures, for any values of α_1 and α_2 the real component of Eigen values of the matrix J are negative, so the matrix J is Hurwitz. Note that the maximum value of real component of these Eigen values are $real(\lambda_1)_{max} = -1.3185$ and $real(\lambda_2)_{max} = -5.1930$.

In addition, since stability of equilibrium point has been proven independent to the values of external disturbances, robust stability of closed-loop car-like robot system is proven as well.

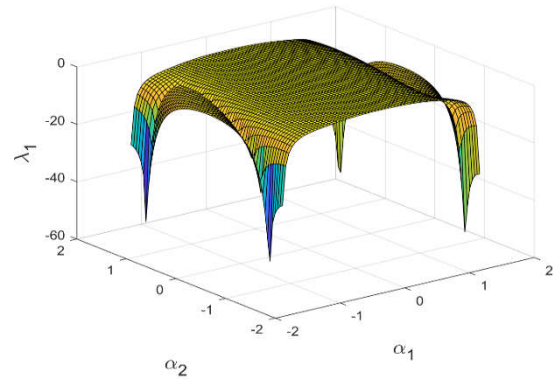


Fig. 4. Real component of the first Eigen value (λ_1) of the matrix J in terms of α_1 and α_2

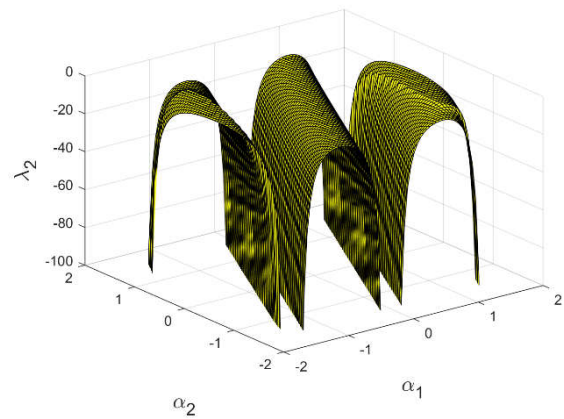


Fig. 5. Real component of the second Eigen value (λ_2) of the matrix J in terms of α_1 and α_2

4. Simulation Results

In this section, simulation result of car-like robot path following in the presence of sliding effect will be presented and responses of suggested controller as well as MISO PI controller will be investigated. Note that, all simulations are done by MATLAB Simulink and utilizing nonlinear model of car-like robot (3). Moreover, three different path is considered including linear, square, and sine function path. Note that in all following simulations, values of sliding effect angles are defined as $\alpha_1 = 5^\circ$ and $\alpha_2 = 5^\circ$.

4.1. Linear Function Path Test

Line is the simplest route which usually is defined as the first path to investigate the path following performance. Likewise, first path in this paper is considered the line $f(x) = x$.

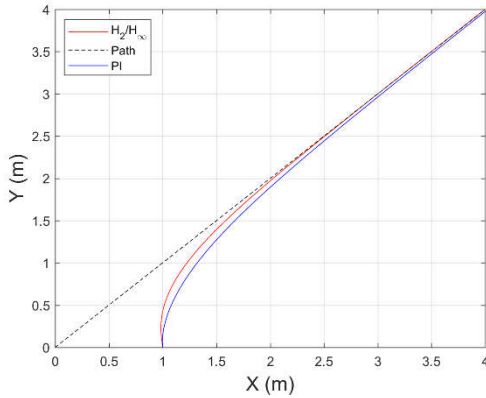


Fig. 6. Path following result for line path

As is shown in Figure 6, car-like robot gradually tends to desired path and after reaching to this path follows it with both mixed H_2/H_∞ and MISO PI controller. In other word, states of path following system tend to their stable values. As is obvious in Figure 6, convergence time and accuracy of mixed H_2/H_∞ is significantly better than PI controller. Note that, this robot was initiated at the point $[x_0 \ y_0] = [1 \ 0]$ with initial heading angle $\psi_{h_0} = \pi/2$.

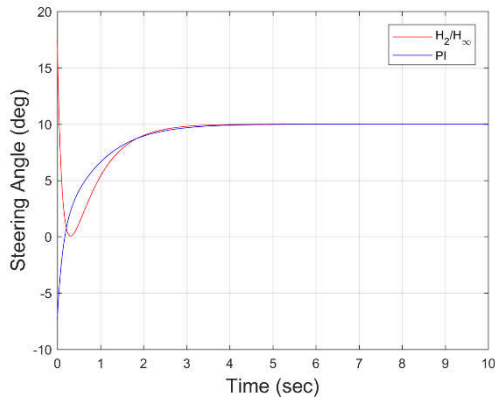


Fig. 7. Control signal for linear path following test

One of the most important parameter in car-like path following is to mind the physical limitation of steering angle. Since this limitation is usually defined as $-\frac{\pi}{2} < \varphi < \frac{\pi}{2}$, both controllers fulfil these constraints well, as is observed from Figure 7. It is worth noting that, although it is generally believed that steady value of steering angle in linear path following should be equal to zero (or should fluctuates around zero), this statement is not valid in the presence of

sliding effect. Thus in this test, steering angle settled on 10° to compensate the sliding effect.

Path following controller is designed to navigate a car-like robot on a desired path, in other word, asymptotically stabilizes path following errors at the origin. As a matter of fact, in the presence of sliding effect stabilization of yaw error at the origin is impossible due to nonholonomic structure of car-like robot. Which means, to deal with sliding effect yaw error must not be stabilized at the origin, as shown in Figure 8. For more details and mathematical analyze of this phenomenon readers are referred to **Appendix B**.

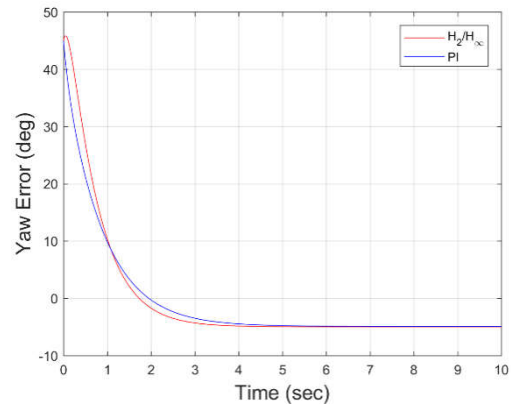


Fig. 8. Yaw error in linear path following test

Figure 9 also shows the accurate path following, since position error gradually tends to zero. Moreover, position error in steady state is less than 3mm for mixed controller, however, it is about 8mm for PI controller. Thus, the accuracy of suggested path following controller to track a linear path even in the presence of sliding effect is proven.

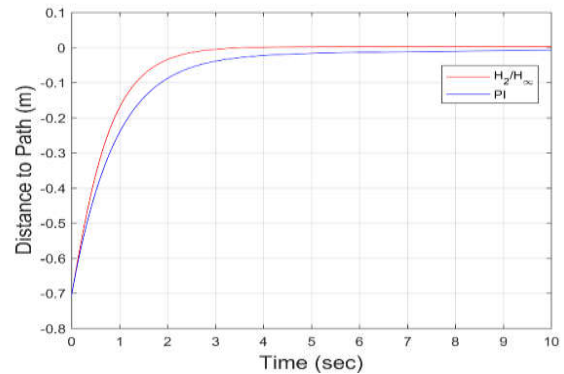


Fig. 9. Position error in linear path following test

4.2. Square Function Path Test

Square function path is used in second test to investigate the performance of the path following controller in more complex situation. In this article the square function path is defined as $y = x^2$.

As can be viewed from Figure 10, both mixed H₂/H_∞ and MISO PI path following controllers are able to manipulate car-like robot to follow square function path. However, mixed H₂/H_∞ controller is faster and more accurate than the PI controller. In this test, robot was initiated at $[x_0 \ y_0] = [-2 \ 3]$ with initial heading angle $\psi_{h_0} = -\pi/2$.

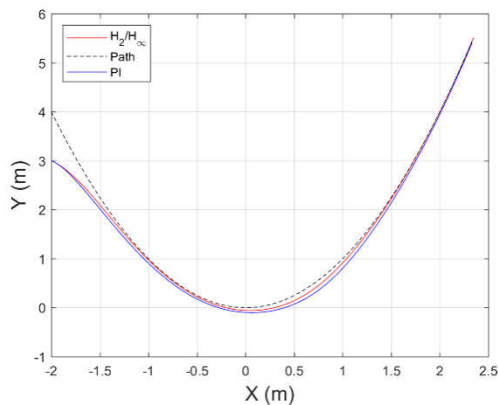


Fig. 10. Path following result for square function path

Control signals in square function path test satisfy the physical limitation of car-like robot with both controllers according to the results which are shown in Figure 11. It is worth noting that, although mixed H₂/H_∞ controller is faster and more accurate than PI controller, these advantages does not achieve by huge amount of control effort, as is obvious in Figure 11.

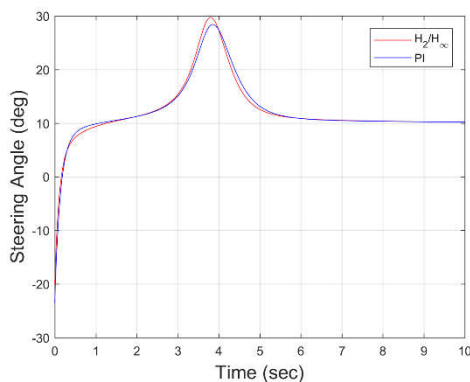


Fig. 11. Control signal for square function path following

Based on the results that are presented in Figures 12 and 13, mixed H₂/H_∞ controller not only is better than PI controller in accuracy and speed of convergence, but this controller also navigates car-like robot with less yaw error.

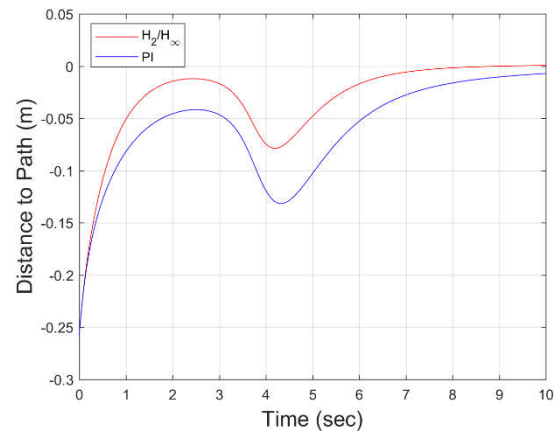


Fig. 12. Position error in square function path following

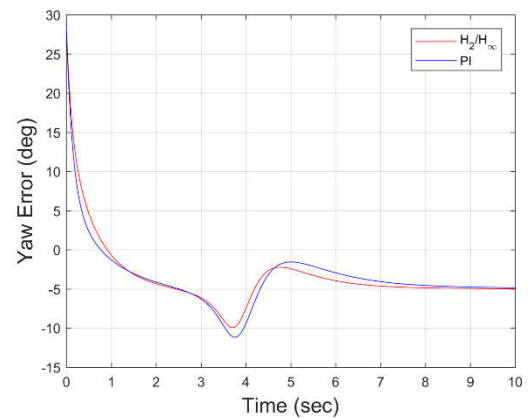


Fig. 13. Yaw error in square function path following test

4.3. Sine Function Path Test

Complexity of a path, especially when navigation is done by path following approaches, depends on the curvature of the path. For instance, linear path which its curvature is zero is the simplest path for investigation of a path following controller. The next path, which is usually is used in the article in field of path following like [17], is circle because its curvature is a non-zero constant number. However, some path such as sine function path are significantly more complex than the circle paths due to the

fact that, the curvature in sine path is not a constant number and continuously varies.

Therefore, in this paper sine function path is chosen to investigate the performance of suggested path following controller. In this article the sine function path is defined as $y = \text{Sin}(x)$.

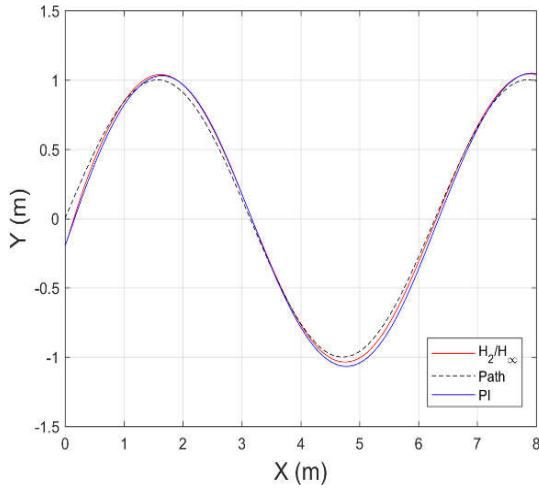


Fig. 14. Path following result for sine function path

Car-like robot with both mixed H_2/H_∞ and MISO PI path following controllers is able to follow complex path such as sine function path based on Figure 14. Although around the optimum points of the sine function path, where the value of curvature rapidly changes, position error increases for both controllers, sine function path is followed. As is realized from Figure 14, accuracy and convergence speed of mixed H_2/H_∞ controller is higher than PI controller. Note that, in this test car-like robot was initiated at $[x_0 \ y_0] = [0 \ -0.2]$ with initial heading angle $\psi_{h_0} = \pi/4$.

As shown in Fig. 15, neither mixed H_2/H_∞ controller nor MISO PI controller does not cross the physical limitation of car-like robot. In Figure 15 it is seen that, control signals are not noticeably different. Therefore, accurate and fast response of mixed H_2/H_∞ is not obtained by utilizing more control effort and this accuracy is one of the most important intrinsic advantages of suggested controller.

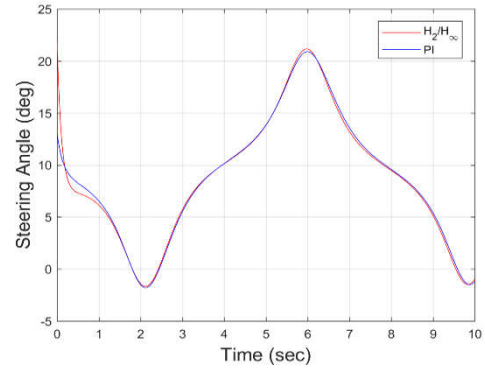


Fig. 15. Control signal for sine function path following

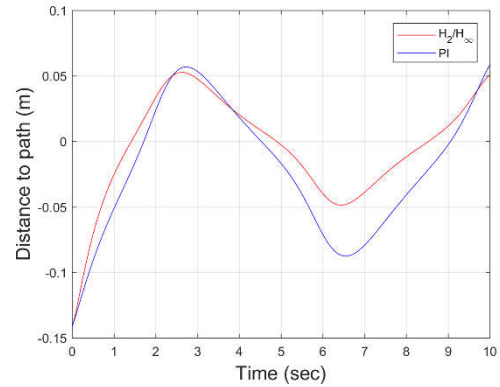


Fig. 16. Position error in sine function path following

Robot position error and yaw error are increased simultaneously with rapid change in path curvature for H_2/H_∞ and MISO PI path following controllers, as shown in Figures 16 and 17. However, response of mix H_2/H_∞ controller is noticeably better than PI controller.

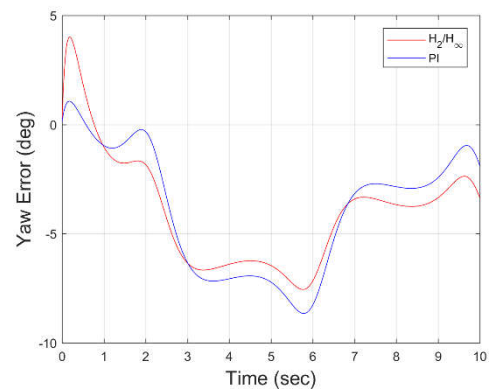


Fig. 17. Yaw error in sine function path following

5. Conclusion

In this paper, robust mix H_2/H_∞ static state feedback control method has been presented as a solution to car-like robot path following problem. Since the robustness to sliding effect is a significant aspect of car-like robot path following controller, robust performance of proposed controller against sliding effect has been investigated in different cases including: following linear, square, and sine function path; and in comparison with a PI controller. As a result of these tests, which have been done by MATLAB Simulink, robustness to sliding effect has been proven as well as accurate path following performance of suggested controller.

For future works, we suggest some improvements to achieve a more accurate model, which consists of a term to model the exact behavior sliding effect when car-like robot moves on sandy surface. Because the existing research that has been used in numerous articles, modeled the behavior of sliding effect on the roads, some modification of car-like robot to move on sandy surface and making dynamic models must be necessary.

APPENDIX A

EQUILIBRIUM POINT CALCULATION AND SYSTEM LINEARIZATION

To find the equilibrium point of car-like robot path following system (6), first it is assumed that, all the system inputs including external disturbances and control input are equal to zero. Based on these assumption, system (6) is represented as (17).

$$\begin{cases} \dot{e} = v_x \sin \psi \\ \dot{\psi} = 0 \end{cases} \quad (17)$$

Then by defining $\dot{X} = 0$, equilibrium points $X_{eq} = [e_{eq} \ \psi_{eq}]$ of the system are calculated.

$$v_x \sin \psi_{eq} = 0 \Rightarrow \psi_{eq} = k\pi \quad k = 0, 1, \dots \quad (18)$$

Since there is not any constraints on e_{eq} , the value of this state is free and any real values is acceptable as e_{eq} . Therefore, equilibrium point of car-like robot path following is chosen as $[e_{eq} \ \psi_{eq}] = [0 \ 0]$.

Linearization of the car-like robot path following system around its equilibrium point is done based on *Jacobian Linearization Technique* as following.

$$\begin{cases} F_1 = v_x \sin \psi + v_x \tan \alpha_1 \cos \psi \\ F_2 = v_x \frac{\tan(\varphi - \alpha_2) - \tan \alpha_1}{L} - \rho_{(\sigma)} v_x \end{cases} \quad (19)$$

$$\begin{aligned} \dot{e} = & \left(\frac{\partial F_1}{\partial e} \right)_{x_{eq}} e + \left(\frac{\partial F_1}{\partial \psi} \right)_{x_{eq}} \psi + \left(\frac{\partial F_1}{\partial \varphi} \right)_{x_{eq}} \varphi \\ & + \left(\frac{\partial F_1}{\partial \alpha_1} \right)_{x_{eq}} \alpha_1 + \left(\frac{\partial F_1}{\partial \alpha_2} \right)_{x_{eq}} \alpha_2 \\ & + \left(\frac{\partial F_1}{\partial \rho} \right)_{x_{eq}} \rho \end{aligned} \quad (20)$$

$$\begin{aligned} \dot{\psi} = & \left(\frac{\partial F_2}{\partial e} \right)_{x_{eq}} e + \left(\frac{\partial F_2}{\partial \psi} \right)_{x_{eq}} \psi + \left(\frac{\partial F_2}{\partial \varphi} \right)_{x_{eq}} \varphi \\ & + \left(\frac{\partial F_2}{\partial \alpha_1} \right)_{x_{eq}} \alpha_1 + \left(\frac{\partial F_2}{\partial \alpha_2} \right)_{x_{eq}} \alpha_2 \\ & + \left(\frac{\partial F_2}{\partial \rho} \right)_{x_{eq}} \rho \end{aligned} \quad (21)$$

Therefore, the linear representation of the system is calculated as (12).

APPENDIX B

EQUILIBRIUM POINT OF CAR-LIKE ROBOT PATH FOLLOWING SYSTEM IN THE PRESENCE OF SLIDING EFFECT

Although it is usual to omit all external disturbances to find the equilibrium point of a system for system linearization, it is possible to face stabilization of the system at another equilibrium point of the system in the presence of external disturbance. This phenomenon is happened in the systems which have more than one equilibrium point, like car-like robot path following system. Therefore, in this section the equilibrium point of car-like robot path following system is calculated in the presence of external disturbances.

To find equilibrium point $X_{eq} = [e_{eq} \ \psi_{eq}]$, it is defined that $\dot{X} = 0$

$$\dot{e} = 0 \Rightarrow v_x \sin \psi_{eq} + v_x \tan \alpha_1 \cos \psi_{eq} = 0 \quad (22)$$

$$\Rightarrow \sin \psi_{eq} + \tan \alpha_1 \cos \psi_{eq} = 0$$

$$\Rightarrow \psi_{eq} = -\alpha_1$$

$$\dot{\psi} = 0 \Rightarrow v_x \frac{\tan(\varphi - \alpha_2) - \tan \alpha_1}{L} - \rho_{(\sigma)} v_x = 0 \quad (23)$$

Since there is not any constraints on e_{eq} , the value of this state is free and any real values is acceptable as e_{eq} . Therefore, equilibrium point of car-like robot path following in the presence of external disturbances is defined as $[e_{eq} \ \psi_{eq}] = [0 \ -\alpha_1]$.

References

- [1] Samani, N. N.; Danesh, M.; Ghaisari, J., "Parallel parking of a car-like mobile robot based on the P-domain path tracking controllers," *IET Control Theory and Applications*, vol. 10, no. 5, pp. 564-572 (2016).
- [2] Akhtar, A.; Nielsen, C.; Waslander, S. L., "Path following using dynamic transverse feedback linearization for car-like robots," *IEEE Transactions on Robotics*, vol. 31, no. 2, pp. 269-279 (2015).
- [3] Akhtar, A.; Nielsen, C., "Path following for a car-like robot using transverse feedback linearization and tangential dynamic extension," in *Decision and Control and European Control Conference (CDC-ECC), 2011 50th IEEE Conference on*, pp. 7974-7979: IEEE (2011).
- [4] Chen, B.; Jiao, Z., "Adaptive path following control of car-like mobile robot using dynamic model," in *Industrial Electronics and Applications (ICIEA), 2011 6th IEEE Conference on*, pp. 239-244: IEEE (2011).
- [5] Abatari, H. T.; Tafti, A. D., "Using a fuzzy pid controller for the path following of a car-like mobile robot," in *Robotics and Mechatronics (ICRoM), 2013 First RSI/ISM International Conference on*, pp. 189-193: IEEE (2013).
- [6] Angelova, A.; Matthies, L.; Helmick, D.; Sibley, G.; Perona, P., "Learning to predict slip for ground robots," in *Robotics and Automation, 2006. ICRA 2006. Proceedings 2006 IEEE International Conference on*, pp. 3324-3331: IEEE (2006).
- [7] Cabecinhas, D.; Cunha, R.; Silvestre, C., "A globally stabilizing path following controller for rotorcraft with wind disturbance rejection," *IEEE Transactions on Control Systems Technology*, vol. 23, no. 2, pp. 708-714 (2015).
- [8] Caharija, W., "Integral line-of-sight guidance and control of underactuated marine vehicles: Theory, simulations, and experiments," *IEEE Transactions on Control Systems Technology*, vol. 24, no. 5, pp. 1623-1642 (2016).
- [9] Hu, C.; Jing, H.; Wang, R.; Yan, F.; Chadli, M., "Robust H_∞ output-feedback control for path following of autonomous ground vehicles," *Mechanical Systems and Signal Processing*, vol. 70, pp. 414-427 (2016).
- [10] Jing, H.; Hu, C.; Yan, F.; Chadli, M.; Wang, R.; Chen, N., "Robust H_∞ output-feedback control for path following of autonomous ground vehicles," in *Decision and Control (CDC), 2015 IEEE 54th Annual Conference on*, pp. 1515-1520: IEEE (2015).
- [11] Arogeti, S. A.; Berman, N., "Path following of autonomous vehicles in the presence of sliding effects," *IEEE Transactions on Vehicular Technology*, vol. 61, no. 4, pp. 1481-1492 (2012).
- [12] Wang, D.; Low, C. B., "Modeling and analysis of skidding and slipping in wheeled mobile robots: Control design perspective," *IEEE Transactions on Robotics*, vol. 24, no. 3, pp. 676-687 (2008).
- [13] Wang, R.; Jing, H.; Hu, C.; Yan, F.; Chen, N., "Robust H_∞ Path Following Control for Autonomous Ground Vehicles With Delay and Data Dropout," *IEEE Transactions on Intelligent Transportation Systems*, vol. 17, no. 7, pp. 2042-2050 (2016).
- [14] Boyd, S.; El Ghaoui, L.; Feron, E.; Balakrishnan, V., *Linear matrix inequalities in system and control theory*. SIAM (1994).
- [15] Gahinet, P.; Nemirovskii, A.; Laub, A. J.; Chilali, M., "The LMI control toolbox," in *Decision and Control, 1994., Proceedings of the 33rd IEEE Conference on*, vol. 3, pp. 2038-2041: IEEE (1994).
- [16] Emam, M.; Fakharian, A., "Path following of an omni-directional four-wheeled mobile robot," in *Artificial Intelligence and Robotics (IRANOPEN)*, pp. 36-41: IEEE (2016).
- [17] Emam, M.; Fakharian, A., "Robust path following of a car-like robot in the presence of sliding effect based on LMI formulation," in *Artificial Intelligence and Robotics (IRANOPEN)*, pp. 121-126: IEEE (2017).